NJC

ROYAL SOCIETY OF CHEMISTRY

PAPER

Cite this: *New J. Chem.*, 2020, **44**, 14837

Interaction of *N*-acetylcysteine with DPPC liposomes at different pH: a physicochemical study†

Juan Marcelo Arias, Rafael A. Cobos Picot, María Eugenia Tuttolomondo, Aida Ben Altabef * and Sonia Beatriz Díaz*

Received 12th December 2019,
Accepted 6th July 2020

DOI: 10.1039/c9nj06167c

rsc.li/njc

The *N*-acetylcysteine (NAC) is a commonly used mucolytic and antioxidant agent. The knowledge of interactions of the NAC with cell membranes is important to understand its mechanism of pharmacological action at the molecular level. To gain a deeper insight into analyzing *N*-acetylcysteine interactions with multilamellar liposomes of 1,2-dipalmitoyl-*sn*-*glycero*-3-phosphocholine (DPPC) in hydrated states at different pH, we performed experimental studies by differential scanning calorimetry (DSC), Fourier transform infrared spectroscopy (FTIR), and Raman spectroscopy. The behavior of the asymmetric stretching band of the PO_2^- group was studied by FTIR following the changes that occur in the shape of this band in the pretransition and transition stages from the gel state to the crystalline liquid state. The values of the pretransition temperature (T_p) for different molar ratios of the complex at the two pH values studied were coincident between the measurements by FTIR and DSC, with the results reaffirming the importance of the PO_2^- group as a sensor not only in the state of hydration but also in the formation of new intermolecular bonds, which lead to the formation of different domains. The vibrational behavior of the groups of the polar head of the lipid revealed the role of the lipid as an oxidant on the thiol site of the NAC. The results of these studies provide information on membrane integrity and its physicochemical properties. In this aspect, this work has novelty and practicality in pharmacology and analytical chemistry.

INQUINOA-CONICET, Cátedra de Fisicoquímica I, Instituto de Química Física, Facultad de Bioquímica, Química y Farmacia, Universidad Nacional de Tucumán, San Lorenzo 456, T4000CAN S. M. de Tucumán, R., Argentina. E-mail: sonia.diaz@fbqf.unt.edu.ar

† Electronic supplementary information (ESI) available: Effect of NAC on the CH_2, CH_3 vibrational bands and CH_2 deformation band in gel (A) and liquid crystalline phase (B), at pH 2 and at 30 °C and 50 °C respectively by FTIR measurements (Table S1); Effect of NAC on the CH_2, CH_3 vibrational bands and CH_2 deformation band in gel (A) and liquid crystalline phase (B), at pH 7 and at 30 °C and 50 °C respectively by FTIR measurements (Table S2); Bandwidth of the CH_2 antisymmetric and symmetric stretching modes as a function of the molar ratio of NAC : DPPC in gel and liquid crystalline states (Table S3); Effect of NAC on the CH_3, CH_2 stretching vibrational bands, CH_2 deformation and torsion bands and C–C stretching vibration bands by Raman measurements in gel state (Table S4); Intensity ratio of the bands corresponding to the stretching methyl, methylene and carbon–carbon, as a function of the molar ratio of NAC : DPPC in gel state, at pH 2 and 7 (Table S5); C═O stretching mode by FTIR measurements in gel (30 °C) and liquid crystalline (50 °C) states (Table S6); Effect of NAC on the C═O stretching mode by FTIR measurements in gel (30 °C) and liquid crystalline (50 °C) states (Table S7); PO_2^- stretching mode by FTIR measurements and effect of NAC on the PO_2^- stretching modes in gel (30 °C) and liquid crystalline (50 °C) states (Table S8); PO_2^- stretching mode by FTIR measurements and effect of NAC on the PO_2^- stretching modes (Table S9); Calorimetric parameters analyzed for the different samples studied; T_m: transition temperature; ΔH_{cal}: transition enthalpy; $\Delta T_{1/2}$: mean height width of the principal transition; T_p: pretransition temperature and ΔHT_p: pretransition enthalpy (Table S10); Changes in the wavenumber of the CH_2 symmetric stretching in NAC : DPPC (at different molar ratios) liposomes as a function of the temperature (at pH 2 (upper) and 7 (down)) (Fig. S1); FTIR spectra for the stretching modes of the $\nu_{as}CH_2$ and ν_sCH_2 groups, for pure DPPC and NAC : DPPC (all molar ratio), in the gel (A and B) and liquid crystalline (C and D) states (Fig. S2); FTIR spectral bands of carbonyl groups of NAC:DPPC in gel state (30 °C) at pH 2 (A) and at pH 7 (B). The black line represents the contours of the spectra acquired and the blue and red lines represent our estimates of the position and relative intensities of the component bands after deconvolution and fitting (Fig. S3); FTIR spectral bands of carbonyl groups of NAC:DPPC in liquid crystalline state (50 °C) at pH 2 (A) and pH 7 (B). The black line represents the contours of the spectra acquired and the blue and red lines represent our estimates of the position and relative intensities of the component bands after deconvolution and fitting (Fig. S4); FTIR spectra corresponding DPPC liposomes lyophilized and hydrated in the region of the stretching mode of the phosphate group (Fig. S5); Wavenumber *vs.* temperature corresponding DPPC liposomes hydrated in the region of the asymmetric stretching mode of the phosphate group, from the FTIR spectra (upper). First derivative of the values of $\nu_{as}PO_2^-$ *versus* temperature (down) (Fig. S6). See DOI: 10.1039/c9nj06167c

1. Introduction

The aim of this work was to study the interaction of the *N*-acetylcysteine (NAC) with the 1,2-dipalmitoyl-*sn-glycero*-3-phosphocholine (DPPC). Some previous works have been reported using different techniques to study interactions of the cysteine with DPPC, but little effort has been put into investigating how the NAC interacts with lipid bilayers.[1,2] Chemically, the NAC is a derivative of the cysteine. The presence of the acetyl moiety, however, reduces reactivity of the thiol compared with that of the cysteine. For this reason, the NAC is less toxic, less susceptible to oxidation (and dimerization), and is more soluble in water, making it a better source of the cysteine than its parenteral administration.[3–7] The loss of balance between the antioxidant defense and oxidant production in the cells, commonly occurs as a secondary feature in many human diseases and is loosely termed "oxidative stress". This balance is important to maintain optimal cell function and the intracellular redox environment is more reducing than being oxidative. The loss of antioxidant capacity in an oxidatively stressed cell is, however, mainly due to a decrease in the GSH (glutathione) and/or an increase in the GSSG (glutathione disulfide), because the glutathione (GSH) is most abundant intracellular free thiol. Thus, oxidative stress *in vivo* mainly translates to a deficiency of the GSH and/or its precursor, the cysteine.[8]

Antioxidant supplementation has been studied extensively as a method to counter disease-associated oxidative stress. The cysteine pro drug *N*-acetylcysteine, which supplies the cysteine necessary for the GSH synthesis, has been proven to be more effective in treating disease-associated oxidative stress. The NAC has been used in the clinic to treat a variety of conditions, including drug toxicity (acetaminophen toxicity).[9]

In cystic fibrosis (CF), we recently demonstrated the beneficial effects of oral NAC in CF in a 4 weeks, dose-escalating phase 1 trial. The benefits detected included a reduction of the neutrophil burden in CF airways and a reduction in elastase and interleukin-8 levels in lung fluid.[10] In addition to being an indirect antioxidant, the reducing action of NAC also explains its mucolytic activity due to the effect of NAC in the reduction of strongly cross-linked mucus glycoproteins. This can be explained by its high pK_a value of 9.52 compared to the values of Cys and its derivatives (pK_a ~ 6–8). The reduced acidity of the thiol (SH) site of NAC, on the one hand, makes it more resistant to air oxidation but less potent as a direct oxidant and, on the other hand, explains the greater disulfide reduction capacity of NAC compared to Cys.[11]

For these reasons, it is important to understand how NAC interacts with the lipid bilayers of the cells. Lipids, together with membrane proteins (intrinsic or associated), constitute the skeleton of biological membranes. Due to their intrinsic compositional complexity, the elucidation of appropriate models explaining the optimal links between the structure and function in these systems is a very active area of research, where the importance of lipids in cell function and health is becoming increasingly recognized.[12,13]

The lipid bilayer defects could be ascribed to local changes in the packing of the polar head group due to the difference in hydration of the lipids in the gel and in the liquid crystalline state.[14] In this regard, it is important to bear in mind that the changes of water organization at the lipid interphase could affect the activity of some proteins. Therefore, it would be important in the context of water replacement by H bonding compounds to analyze how NAC interacts with lipids. Thus, it is of interest to analyze the insertion of NAC in lipids at different pHs and hydration states by studying its specific interactions with carbonyl and phosphate groups.

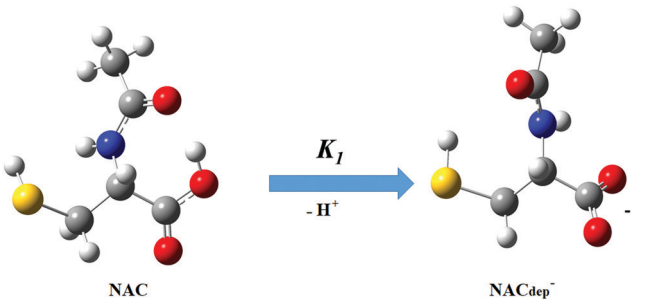

Scheme 1 Dissociation of a proton from the carboxyl group of the NAC (*N*-acethylcysteine), where the deprotonated NAC is called NACdep$^-$ (CO_2^-).

It has been revealed that lipids in their self-organized form are crucial to indirectly control a wide variety of biological functions that occur in or that are directly mediated by the membrane.

New experimental evidence has revealed some unknown functional roles of the lipid component of biological membranes that are as relevant as those assigned to proteins.[12] The values of the T_p for the different molar ratios of the complex at the two pHs studied were coincident between the measurements by FTIR and DSC, and these results reaffirmed the importance of the PO_2^- group as a sensor not only of the state of hydration but also of the formation of new intermolecular bonds, which would lead to the formation of different domains. Therefore at acidic pH, when the T_p decreases, we think that there would be an increase in domains in the gel state, while at physiological pH, a greater amount of domains in the crystalline liquid state should be observed.

Scheme 1 illustrates a route for deprotonation of the NAC at different pHs. Between pH 1–2.5 the molecule is in its acid form as NAC. From pH 2.5, the deprotonation of a COOH group (the deprotonated form of NAC is called NACdep$^-$ (CO_2^-)) begins. It should be noted that between pH 2.5–3, both species coexist.

For this purpose, a detailed analysis by FTIR was performed in the gel and in the fluid state of the aqueous suspension of DPPC (1,2-dipalmitoyl-*sn-glycero*-3-phosphocholine) at different NAC/lipid ratios. Different approaches were used to understand and explain the complex interactions of NAC with the fully hydrated liposomes of DPPC, including by infrared spectroscopy (FTIR), Raman microscopy, and differential scanning calorimetry (DSC).

2. Experimental

2.1. Lipids and chemicals

Synthetic 1,2-dipalmitoyl-*sn-glycero*-3-phosphocholine (DPPC) with a purity of >99% and *N*-acetylcysteine were purchased

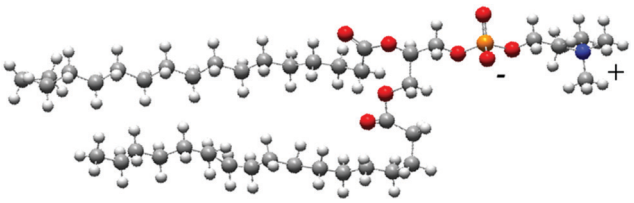

1, 2 dipalmitoyl-sn-glycero-3-phosphocholine

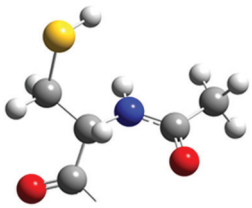

N-Acetylcysteine

Scheme 2 Chemical structures of 1,2-dipalmitoyl-*sn-glycero*-3-phosphatidylcholine (DPPC) and *N*-acetylcysteine molecules used in this study.

from Sigma-Aldrich Inc. (St Louis, MO, USA). The purity was checked by thin layer chromatography and the lipids were used without further purification. The *N*-acetylcysteine (NAC) purity was checked by FTIR spectroscopy (Scheme 2). 1 M NaOH was added dropwise in order to obtain a solution at pH 7, corresponding to zwitterionic species with protonated (–SH) and deprotonated carboxylic groups ($-CO_2^-$). All the other chemicals were of analytical grade. Milli-Q water was employed in all the experiments.

2.1.1. Multilamellar vesicles preparation. Multilamellar vesicles (MLVs) were prepared following Bangham's method[15] to study the NAC and DPPC interaction. The phospholipids in chloroform solutions were dried under a nitrogen stream to form a homogeneous film that was left for 24 h under vacuum to ensure proper solvent removal. The pure lipids were rehydrated and resuspended by vortexing in de-ionized, water (Milli-Q), and in D_2O. Liposomes of the NAC:DPPC complexes were formed by resuspending the pure lipid in solutions of different concentrations of NAC in H_2O (Milli-Q) and in D_2O (25, 75, 100, and 200 mM) at 10 °C higher than the lipid transition temperature (T_m = 41.5 °C). Mechanical dispersion of the hydrated lipid film was achieved under vigorous shaking for 15 min, resulting in an opalescent suspension of multilamellar vesicles (MLVs). The final concentration of the MLVs was 50 mg mL^{-1}. The anhydrous samples were prepared by lyophilization.

2.1.2. FTIR measurements. FTIR measurements were carried out in a PerkinElmer GX spectrophotometer provided with a DTGS detector constantly purged with dry air. NAC interactions with the phospholipid head groups and hydrocarbon chains of the hydrophobic region in the hydrated state were studied by dispersing the lipid and NAC:DPPC samples at different molar ratios in D_2O first and then in H_2O. The spectra were acquired in a demountable cell with a ZnSe window for the liquid samples. The cell temperature was controlled using a Peltier-type system with an accuracy of ±0.5 °C. The resolution of the equipment employed was 1 cm^{-1}. All the samples were left at room temperature for 1 h before the measurements. The working temperature range was 30 °C to 50 ± 0.5 °C. Experiments were repeated three times and the spectra of the samples were collected at the aforementioned temperatures. A total of 256 scans were done in each condition and the spectra were analyzed using the OMNIC v.7.2 mathematical software provided by the manufacturer. The mean values of the main bands in each condition (acid and physiological pH values) were obtained from a total of three different batches of samples. The standard deviation of the wavenumber shift calculated from this pool of data was about ±1.5 cm^{-1} in all the conditions assayed.

The Fourier self-deconvolution algorithm was applied to define the contours of overlapping bands. Accurate wavenumbers of the center of gravity of C=O stretching component bands were obtained by using the bandwidth parameters between 18 and 20 cm^{-1} and the band narrowing factors 1.6–2.2, followed by curve fitting to obtain the band intensities.

The shifts of these two populations were studied as a function of NAC concentration in the gel ($L_{\beta'}$) and liquid crystalline phases (L_α).

The bands of the normal modes corresponding to the C=O and PO_2^- groups of the NAC:DPPC complex were assigned in comparison with the spectra of the pure lipid and NAC in the aqueous solution. NAC/DPPC spectra were obtained by dispersing the lipid in NAC aqueous solutions, from which the spectrum of pure NAC aqueous solution was subtracted.

2.1.3. Raman measurements. The vibrational Raman spectra of DPPC dispersed in NAC aqueous solution were recorded using a confocal Thermo Scientific DXR Raman microscope equipped with a high-resolution motorized platen, a set of Olympus optical objectives, a lighting module bright-field/dark-field trinocular viewer, an Olympus camera of 2048 pixels with a charge-coupled device detector, and an OMNIC Atlμs mapping software with advanced features cooled by a Peltier module. The confocal system was real, with an opening/hole matched with the point of symmetry of the excitation laser. The standard spatial resolution was better than 1 μm.

The samples were placed on gold-coated sample slides. In order to achieve a sufficient signal-to-noise ratio, 100 acquisitions with an exposure time of 5 s were accumulated for all the samples. The laser power was set at 10 mW, and the laser wavelength was 532 nm. Water solutions of NAC were measured with the Thermo Scientific DXR Smart Raman spectrometer. The liquid sample was placed in a glass cuvette. All the spectroscopic experiments were carried out at ambient temperature. The spectra were analyzed using the OMNIC™ program for dispersive Raman.

2.1.4. DSC measurements. Calorimetry was performed on a PerkinElmer DSC6 differential scanning calorimeter. A scan rate of 2 °C min^{-1} was used for all the samples. The sample runs were repeated at least three times to ensure reproducibility.

Data acquisition and analysis were done using data from DSC by integrating the peak with Pyris 6 software, provided with the set, and Origin software (Microcal). The total lipid concentrations used for the DSC analyses were about 50 mg mL^{-1}

for full hydration for the NAC–DPPC mixtures, containing about 20 g H_2O/1 g lipid.[16,17] The experiments were carried out using 20 μL sealed in aluminum sample pans. The instrument was calibrated with indium standard samples. The enthalpy changes associated to the phase transition temperatures of the samples (ΔH) were obtained from the DSC data by integrating the peak using the Pyris 6 software provided with the set. The entropy changes related to phase transition were finally determined with the relation $\Delta S = \Delta H/T$.

Table 1 Phase-transition temperature for different molar ratios: NAC : DPPC in H_2O from the FTIR spectra

NAC : DPPC molar ratio	pH 2 T_m (°C) H_2O	pH 7
0.00 : 1.0	41.6	41.6
0.37 : 1.0	42.1	40.0
1.10 : 1.0	41.6	43.7
1.47 : 1.0	41.9	43.0
2.93 : 1.0	41.8	43.8

3. Results and discussion

3.1. Hydrophobic region

The hydrophobic region corresponding to the hydrocarbon chains was analyzed by various spectroscopic techniques, such as Fourier transform infrared (FTIR) spectroscopy and Raman microscopy and by thermal techniques, like differential scanning calorimetry (DSC) in order to study how this region was modified in its interaction with NAC. In addition, the spectroscopic analysis results were used to characterize the phase changes of the NAC complex: DPPC.

3.1.1. FTIR measurements. FTIR studies were carried out to monitor the effect of the acyl chain length on the NAC/DPPC interaction. The CH_2 antisymmetric and symmetric stretching vibrations were located at 2919 and 2850 cm^{-1}, respectively. The thermal phase transition could be monitored by following the changes in the wavenumber of the band corresponding to the symmetrical stretch of the CH_2 group. This band is sensitive to temperature changes and can be used to determine the transition temperature (T_m) of the lipid by FTIR, because of its sensitivity to the changes in mobility in the conformational disorder of hydrocarbon chains. These changes increase as the acyl chains melt and the number of *gauche* conformers increases.[18–20] The order–disorder state of the system was investigated by wavenumber analysis of the CH_2 stretching modes.[21]

Fig. S1 (ESI†) shows the temperature of transition (T_m) for the pure DPPC and for the mixtures with NAC at pH 2 and 7. These values were determined with the first derivative of the curve obtained by plotting the wavenumber of the symmetric stretching of the CH_2 group as a function of the sample temperature.

In the literature, the value of the temperature of transition is 41.5 °C for the pure DPPC. Our FTIR study revealed a transition temperature of 41.6 °C for pure DPPC and a slight increase in T_m of the NAC:DPPC complexes at different molar ratios and pHs (Table 1).

It was observed at the molar ratio 0.37 : 1.00 at pH 7 that T_m decreased with respect to the value at pH 2. This reveals a different behavior in the distribution of NAC in the different domains of the membrane at physiological pH, promoting the formation of crystalline liquid domains.

At higher concentrations of NAC and at acidic pH, no alteration of T_m was observed, indicating that NAC did not interact with the membrane at the hydrophobic level; while an increase in concentration at physiological pH produced stabilization of the gel phase.

The wavenumber changes of the symmetric and antisymmetric stretching vibrations of the CH_3 and CH_2 groups and deformation bands of the CH_2 group inside the lipid bilayer were not significant within experimental error in both the gel and liquid crystalline phases (Tables S1 and S2, ESI†).

The dynamic state of the system was studied by monitoring the bandwidth values of the CH_2 antisymmetric stretching mode at 0.50 peak height (HWHH-half width at half height), for different molar ratios of NAC : DPPC in both the gel and liquid crystalline states at different pH values.

The concentration-dependent variations in bandwidths reflect changes in the mobility of the acyl chains. The increase in bandwidth is associated with an increase in the lateral mobility of the lipid acyl chains, while the wavenumber shift is related to the introduction of *gauche* conformers in the hydrocarbon chains.[21–26] In other words, the membrane fluidity is heightened by an increase in the rates of lateral diffusion of the lipid molecules.

In Fig. 1, we can see the changes in the bandwidth values or membrane fluidity[27] as a function of the concentration of NAC:DPPC for the νCH_2 antisymmetric stretching mode in both the gel and liquid crystalline phases. Fig. 2 shows the comparison between DPPC pure and 1.10 : 1.00 molar ratio at acid and physiological pH in both the gel and crystalline liquid states. It can be seen that for the ν_{as} CH_2 group at pH 7, the behavior is

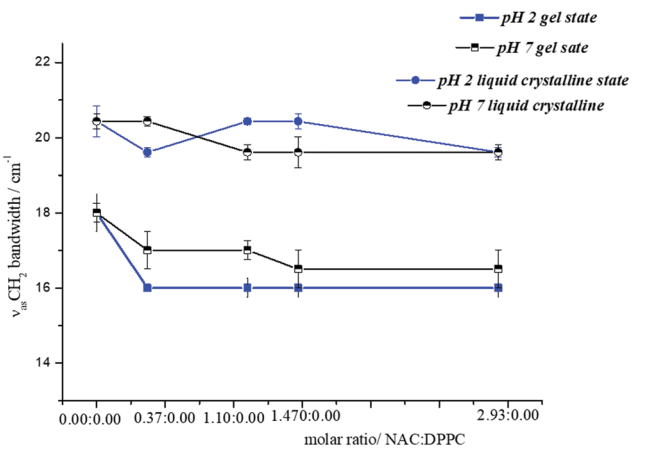

Fig. 1 Bandwidth of the CH_2 antisymmetric stretching mode as a function of the molar ratio of NAC : DPPC in the gel and liquid crystalline states at different pH values.

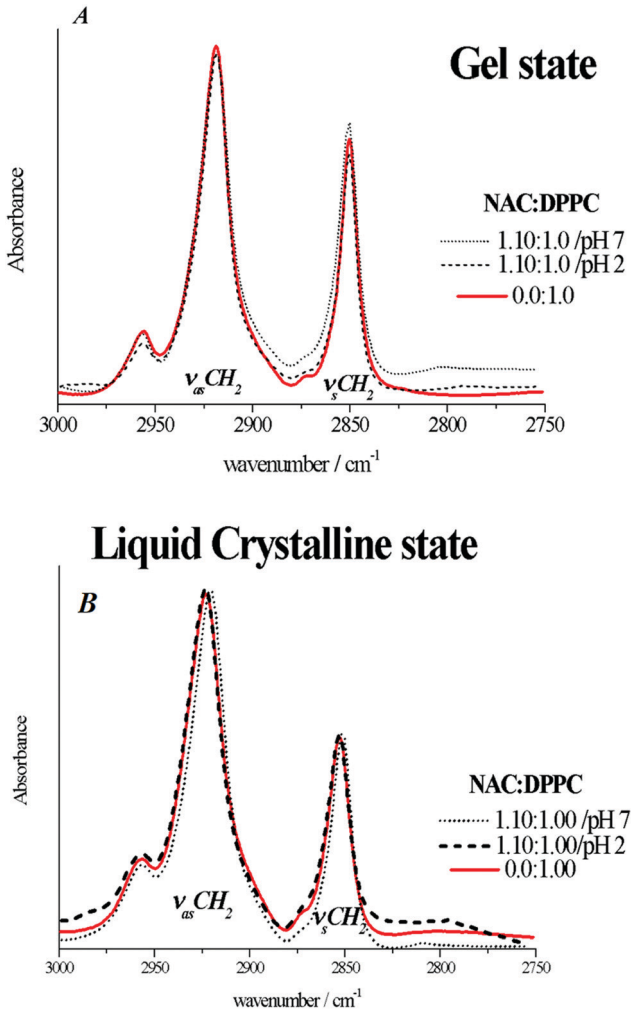

Fig. 2 FTIR spectra of NAC : DPPC at 1.10 : 1.00 molar ratio in the 3000 cm^{-1} region in the gel state (A) and in the liquid crystalline state (B).

not monotonic, showing a slight decrease in the bandwidth at all molar ratios compared to pure DPPC; while at pH 2, the bandwidth or membrane fluidity does not vary with respect to the pure lipid. Similar results were also observed for the liquid crystalline state (Table S3, ESI†).

It can be concluded that the observed changes in the bandwidth were within the experimental error. The behavior of fluidity in the membrane would facilitate the mechanism of action of NAC for the pharmacological activity tested.

3.1.2 Raman measurements. The Raman spectrum of a phospholipid is dominated by vibrations of the hydrocarbon chains, with an overlap of a few bands of the head group.[22–25]

By Raman spectroscopy, in the pure DPPC spectrum, three areas corresponding to the hydrocarbon chains could be clearly observed: C–H stretching modes (3000–2800 cm^{-1}), CH_3 and CH_2 deformation modes (1400–1200 cm^{-1}), and a C–C stretching mode (1200–1000 cm^{-1}) (Table S4, ESI† and Fig. 3). The relationships between the intensities of these bands are especially useful for the determination of the different chain forms (Table S4, ESI†).

In the area of the spectrum ranging from 3000 to 2800 cm^{-1}, the corresponding interchain coupling could be seen (generally, wavenumber shifts toward higher values mean an increase in the decoupling of the chains).[23,24]

It should be noted that the pure NAC bands do not interfere at the concentrations used and no excess NAC bands were observed. Furthermore, the DPPC bands analyzed did not overlap with those of pure NAC, particularly in the 3000 cm^{-1} region, where the symmetric stretching band of the CH_3 group of the NAC appeared at 2947 cm^{-1} and the band of the asymmetric stretching C–H of DPPC appeared at 2935 cm^{-1}.

No significant changes were found in the νCH_3 frequencies of the complex with respect to pure DPPC because these displacements were within experimental error (Table S3, ESI†).

The frequencies of the stretching modes of the CH_2 group reflect the conformational order and the coupling between the hydrocarbon chains, and here we could see a shift toward lower frequencies for the CH_2 group stretching modes in contrast with pure DPPC.

The intensity ratio of I_{2881}/I_{2850} ($I_{\nu_{as}CH_2}/I_{\nu s.\,CH_2}$) is a measure of lateral packing density of alkane chains and is itself an indication of order.

The intensity ratio of I_{2881}/I_{2850} is a measure of the lateral packing density of alkane chains and is itself an indication of order. At physiological pH, the NAC:DPPC complex produced a new packing, observed as a decrease in I_{2881}/I_{2850} as the NAC : DPPC molar ratio increased.

According to Orendorf, these changes are due to the rotational disorder of the methyl and methylene groups, predominantly near the ends of the hydrocarbon chains.[22–24] We can see in Fig. 4 and Table S5 (ESI†) that at pH 2, this behavior would indicate that the presence of NAC did not alter the hydrophobic region.

The ratio of intensities between the bands corresponding to the symmetric stretching of the methyl and methylene groups provides information on the coupling of the hydrocarbon chains (Table S5, ESI†). As the chains uncouple (the intermolecular interactions decrease), the terminal methyl group undergoes an increase in free rotation and the intensity ratio I_{2935}/I_{2851} increases.[24,25]

Fig. 4 shows the different intensity ratios studied in the gel state, where we can see there was an increase in the ratio I_{2935}/I_{2851} for different NAC : DPPC molar ratios compared to pure DPPC, which would indicate a decrease in the intermolecular interactions. This behavior was intensified at physiological pH.

The intensity ratio I_{1099}/I_{1066} of the peaks is a parameter indicating the relative number of *gauche*/*trans* rotamers in the acyl chains of the phospholipids. An increase in temperature produces an increase in the ratio *gauche*/*trans*, which indicates a larger population of *gauche* rotamers.[22] Our results revealed a slight increase in the *gauche* rotamers for the different molar ratios of NAC : DPPC in comparison with the pure lipid at both pH values.

As can be seen at physiological pH, a slight increase in the population of *gauche* rotamers was observed, together with a decrease in the I_{2881}/I_{2850} ratio and a slight increase in I_{2935}/I_{2851}.

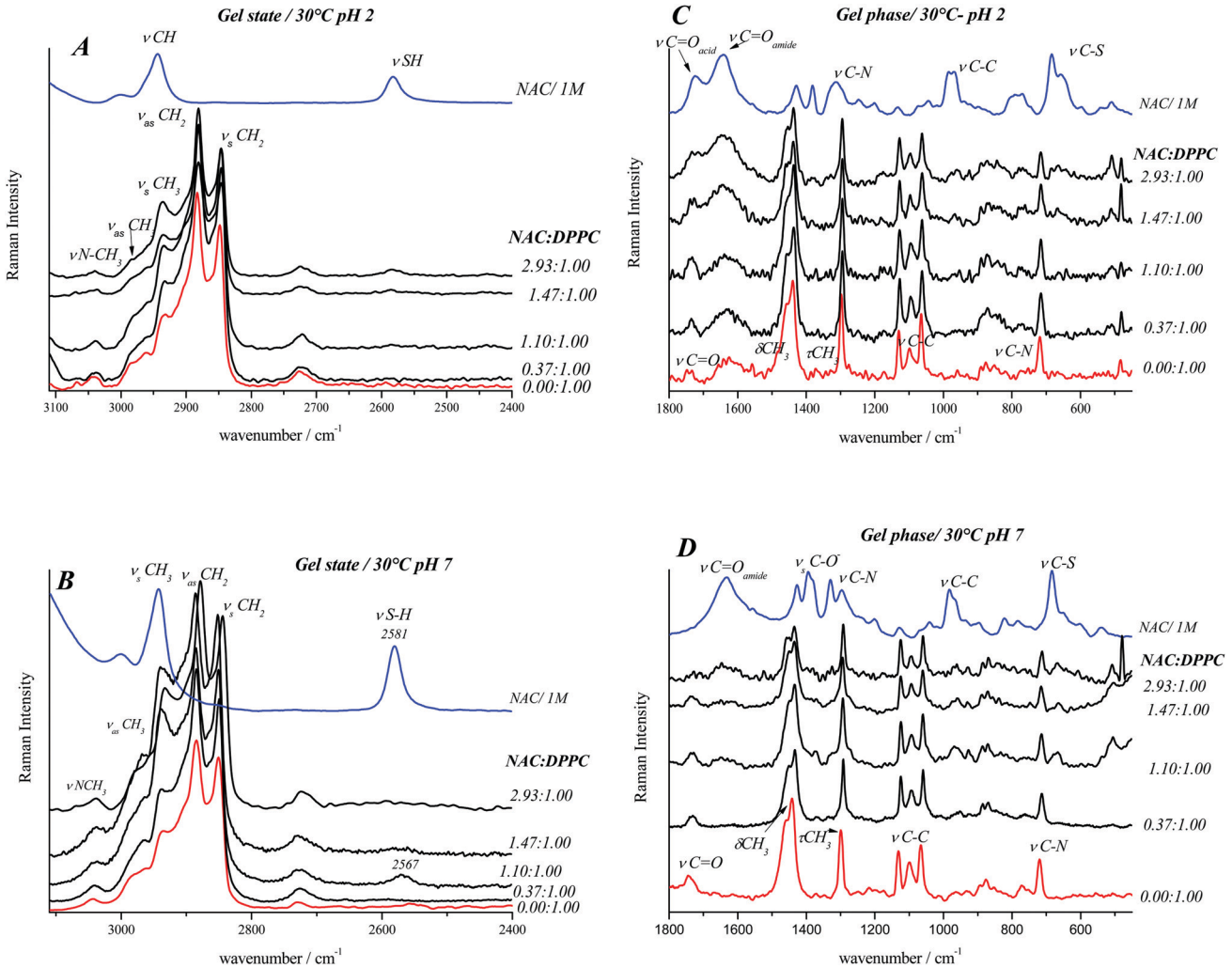

Fig. 3 Raman spectrum of the DPPC, NAC, and different NAC : DPPC molar ratios at pH 2 and 7 in the gel state at 30 °C.

This behavior indicated that a new order occurred in the hydrophobic zone. The non-monotonic behavior of the DPPC:NAC complex is a consequence of the different concentrations of NAC in the bilayer, with it accommodating itself to achieve the greatest stability.

3.2. Hydrophilic region

3.2.1. FTIR measurements. The hydrophilic region is strongly dependent on the state of hydration and is susceptible to hydrogen bonding. The bands were assigned to the carbonyl and phosphate groups by comparison with pure lipids dispersed in D_2O and H_2O, respectively.

Acetylcysteine (NAC) in aqueous solution presents a balance between the different forms in which it is found at different pH values. Scheme 3 shows how NAC interacts with lipid bilayers. Between pH 2.5–3, the deprotonation of the carboxyl group (COO^-) begins. It should be noted that in this pH region, both species coexist (NAC and NAC_{dep}^-). In addition, at pH 7, the thiol group (SH) is approximately 2.5% deprotonated.

For this reason, at pH 2, two bands corresponding to the C═O_{acid} and C═O_{acetyl} groups were observed, which in the IR spectrum of the solid appeared at 1718 and 1590 cm^{-1}, respectively; while at pH 7, we only observed the C═O_{acetyl} band at 1637 cm^{-1}.[11]

Carbonyl group (C═O). There is evidence in the literature that the main νC═O peak in diacyl lipids can be decomposed into at least two components, contributing the νC═O vibrational modes of the H-bonded (bond) or hydrated and non-bonded (free) or non-hydrated conformers of the C═O group.[27] The higher frequency band component (1740–1742 cm^{-1}) was assigned to the free C═O groups (νC═O free), whereas the lower frequency component (~1728 cm^{-1}) was attributed to the vibration of the carbonyl group of H-bonded conformers (νC═O bond).

This band was deconvoluted into three components: νC═O_{free}, νC═O_{bond}, νC═O_{NAC} at acid pH and only two components, νC═O_{free}, νC═O_{bond}, at physiological pH.[9,25–28] The effect of NAC on the two populations of the C═O group of the lipid was studied following the free and H-bonded populations[28–31] at different molar ratios in both the gel and crystalline liquid states at both pH. The frequencies of the band components for the

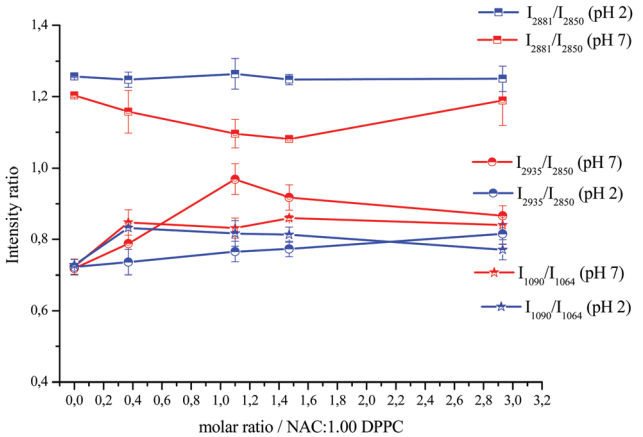

Fig. 4 Intensity ratio of $\nu_a(CH_2)_{2881}$ to $\nu_s(CH_2)_{2846}$, $\nu(C-C)_G$ to $\nu(C-C)_T$; $\nu_s(CH_3)_{2930}$ to $\nu_s(CH_2)_{2846}$ as a function of the molar ratio of NAC:DPPC in the gel state at pH 2 and 7.

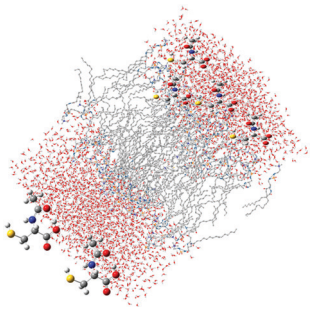

Scheme 3 Scheme of the NAC interactions with the lipid bilayers.[26]

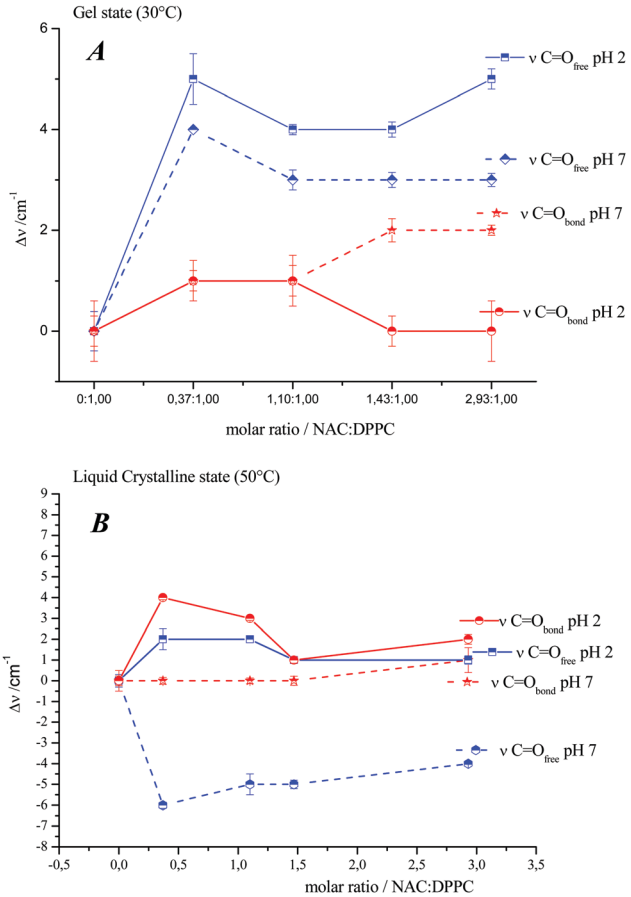

Fig. 5 Wavenumber variation of the CO stretching in connection with the increasing NAC : DPPC molar ratio in the gel (A) and liquid crystalline (B) states at different pH values.

two populations of the carbonyls group were assigned by deconvolution: $\nu C{=}O_{free}$ (1739 cm^{-1}) and $\nu C{=}O_{bond}$ (1724 cm^{-1}) at 30 °C, and $\nu C{=}O_{free}$ (1743 cm^{-1}) and $\nu C{=}O_{bond}$ (1729 cm^{-1}) at 50 °C for pure DPPC in D_2O (Fig. S2, S3 and Table S6, ESI†). The exposure of the carbonyl groups to the aqueous phase was different for each phase state. This could be observed by the asymmetry that is present in the band corresponding to the carbonyl group when it goes from the gel state to the crystalline liquid.[29–32] The two band components $\nu C{=}O_{free}$ and $\nu C{=}O_{bond}$ changed their relative intensity in the presence of NAC in the different states of hydration and at the pH studied. For the pure lipid in the gel state, it was observed that the population corresponded to $\nu C{=}O_{free}$ more intensely than the band corresponding to $\nu C{=}O_{bond}$, whereas this situation was inverted in the liquid crystalline state. For the complex NAC:DMPC in the gel state, at acid pH, the band corresponding to the population of $\nu C{=}O_{bond}$ was more intense than the band corresponding to that of $\nu C{=}O_{free}$, and the same was observed in the crystalline liquid state, except at the molar ratio of 2.20 : 1.00 NAC : DPPC. This same behavior occurred at physiological pH for all the molar ratios tested. (Fig. S2, S3 and Table S6, ESI†).

Fig. 5 shows there was a significant shift of the bands of both populations to higher wavenumbers with the increase in the NAC : DPPC molar ratio at the two operating temperatures: 30 °C (gel state) and 50 °C (liquid crystalline state) (Table S7, ESI†). A displacement toward higher wavenumbers with an increase in the NAC/DPPC molar ratio for both C═O populations was observed in the gel state. This would imply a loss of water molecules, which would be more significant for the $C{=}O_{bond}$ population, reaching a maximum of 9 cm^{-1} for the 0.73 : 1.0 molar ratio. In the liquid crystalline state, the system was more disordered by the effect of temperature, and this disorder caused NAC to remain for less time in the vicinity of the carbonyl groups due to the greater rotation of the C–C bond of the DPPC glycerol. This behavior would suggest a displacement of the hydration water molecules without the subsequent formation of hydrogen bonds NAC···C═O in both the gel and liquid crystalline states at acidic pH.

In the gel state, significant dehydration at acid pH was observed in both populations of the carbonyl group. At physiological pH, there was a slight loss of structured water in the population of the $C{=}O_{bond}$ group and a weak strength interaction with the hydrogen bond formation NAC···DPPC (Fig. 5). In the crystalline liquid state, at acid pH, this behavior was observed in the gel state for both populations of the carbonyl group; while at physiological pH, the population of the free carbonyl group presented an important interaction, suggesting the loss of structured water with the formation of the hydrogen

bonds C═O$_{free}$ ···NAC (Fig. 4).[32–36] The different intensities of the C═O group bands observed were due to the fact that NAC was incorporated in a different way in the different membrane domains, since it exhibited a non-monotonic behavior, as reported in other studies of DPPC:amino acid interactions.[37–45]

Phosphate group (PO_2^-). The region of the infrared spectrum between 1350 and 1000 cm^{-1} (Fig. S4 and Table S8, ESI†) corresponds to the stretching of the phosphate groups.[1,34–37] It is widely accepted that the wavenumber of the PO_2 asymmetric stretching ($\nu_aPO_2^-$) vibration is very sensitive to lipid hydration, mainly because of direct H binding to the phosphate charged oxygen. The hydration of the anhydrous lipids displaces the band related to the asymmetric phosphate stretching to lower frequencies with increasing H-bonding.[34–37]

At low temperatures, the lipids are in the gel state with a rather rigid structure, restricting their mobility. As the temperature increases, a pretransition occurs before the main phase transition, which has to do with the increase in the rotational mobility of the polar heads of the lipids and the appearance of ripples on the surface of the membrane lipid. This behavior can be studied by FTIR following the changes that occur in the asymmetric stretching band of the PO_2^- group (Fig. S4, ESI†). This band changes its shape in each phase transition. This is a result of overlapping with the wagging movements of the CH_2 group.[30,31] In Fig. 6, the FTIR spectra for the DPPC liposomes at different temperatures are presented, in which the changes produced in the shape of the FTIR spectra in the pre-transition and in the transition from the gel state to the crystalline liquid can be clearly observed. Also in Fig. S5 (ESI†), we can see a T_p value of 36.3 °C corresponding to hydrated DPPC liposomes, which was determined with the first derivative of the curve obtained by plotting the wavenumber of $\nu_{as}PO_2^-$ as a function of the sample temperature. This behavior confirmed the relationship of the pretransition temperature with the rotational movement of the polar heads of the lipid in the rippled phase ($P_{\beta'}$).

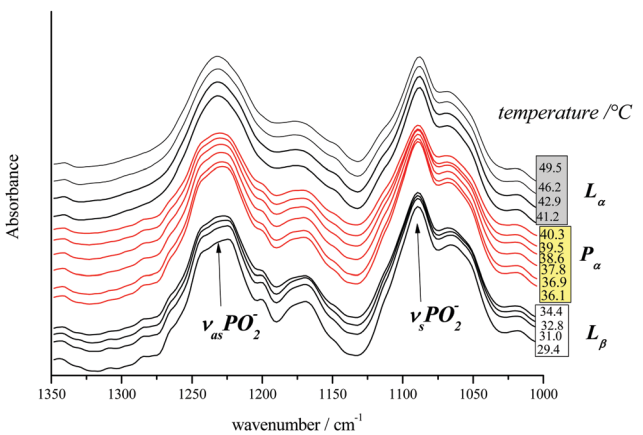

Fig. 6 FTIR spectra corresponding to the DPPC liposomes hydrated in the region of the stretching mode of the phosphate group at different temperatures.

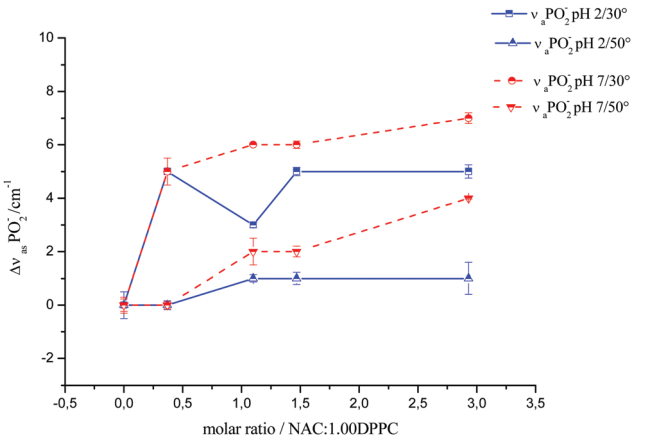

Fig. 7 Infrared spectra of the symmetric and asymmetric PO_2^- stretching vibrational mode as a function of the NAC : DPPC molar ratio in the gel (30 °C) and liquid crystalline (50 °C) states at pH 2 and 7.

Fig. 7 shows the displacements of the band corresponding to symmetric and antisymmetric stretches of the phosphate group for the different molar ratios of NAC : DPPC. In both states, we can see displacements toward higher values of wavenumbers in the two populations ($\nu_aPO_2^-$ and $\nu_sPO_2^-$); this behavior would indicate a moderate dehydration without the subsequent formation of the hydrogen bonds NAC···PO_2^- (Scheme 3).

Table S9 (ESI†) shows the values of the pre-transition temperature for the DPPC and the different molar ratios of DPPC : NAC, both at acid pH and at physiological pH.

At acid pH, a strong decrease in T_p could be observed with the increase in the molar ratio, while at physiological pH, the T_p increased with the increase in the molar ratio of DPPC : NAC. This could be related to the fact that, at acidic pH, the NAC appeared with the protonated carboxyl group and its influence in this region would decrease the energy necessary to pass from one phase to another; while at physiological pH, we find a deprotonated group with a strong electronic density that also produces an inductive effect in the other groups of the NAC molecule, conferring an increased acidity to the thiol group. This site could interact with the PO_2^- group of the membrane, causing an increase in the energy required for the phase change.

Raman measurements. Two bands, clearly identifiable because of the thiol group, may be seen in the Raman spectra of the different NAC : DPPC molar ratios: these are the S–H and C–S stretchings. This band was sensitive to the pH value.[11] Thus, the observed shifts of the S–H stretching band were due to S–H group interactions with some of the nucleophilic groups of the lipid membrane.[36]

S–H, C–N and C–S stretching modes. The S–H stretching mode could be assigned to the band centered at 2548 cm^{-1} in the spectrum of the solid NAC[11] by Raman spectroscopy. In solution, this band appeared at a higher wavenumber (2582 cm^{-1}) because solvation disrupts the intramolecular hydrogen bonding in the crystal. At pH 2, in the NAC:DPPC complex, the value of the wavenumber was maintained, while a decrease was observed in the band intensity. In Fig. 2, we observed that this band (νS–H)

appeared very weakly at 2582 cm^{-1} with the 1.10 : 1.0 to the 2.93 : 1.0 molar ratios, with the increase in intensity directly related to the increase in NAC : DPPC molar ratios. At physiological pH, a shift to a lower wavenumber ($\sim$20 cm^{-1}) would indicate a weakening of the S–H force constant, which was due to a lengthening of the S–H bond because of the formation of a hydrogen bond between NAC with some electronegative groups of the lipid bilayer (Fig. 2).

The presence of a band at 508 cm^{-1} was observed in the Raman spectra at the molar ratios of 0.73 : 1.0, 1.10 : 1.0, and 2.93 : 1.0 with a growing intensity as the NAC : DPPC molar ratio increased. This band was observed in the Cys–Cys dimmer and corresponded to νS–S.[37]

An intense band corresponding to the C–S stretching mode of the NAC water solution at 684 cm^{-1} was observed for all molar ratios in the gel state in the 800–600 cm^{-1} region[36,37] of the C–N and C–S groups.

The interaction of water with the choline groups (N–$(CH_3)_3$ and C–N) has been studied with different phospholipids in the literature. The peaks observed at 3042 and 720 cm^{-1} represent the stretching vibration of the N–$(CH_3)_3$ and C–N bond of the DPPC choline group in the gel state (Fig. 2).

The results of the analysis in the νCH_3 region (Fig. 2 and Table S4, ESI†) revealed a strong interaction between the NAC and the chlorine group with a displacement of the νN–$(CH_3)_3$ frequencies of about 10 cm^{-1}. The intensity changes of the peak at 716–713 cm^{-1} (Table S4, ESI†) indicated a significant interaction between the choline head group and the NAC nucleophilic group, which was of the same strength, regardless of the NAC concentration.

3.3. Differential scanning calorimetry study

The effect of NAC on the membrane phase behavior was determined by DSC. Fig. 8 shows the thermograms of the pure lipid; NAC:DPPC mixture and NAC solution. In this image, we can see the thermal stability of all the compounds in the temperature range (25–70 °C). This indicates that NAC did not decompose at this temperature range and that the endothermic events observed in this study arose exclusively from the phase transitions of the phospholipid vesicles.

DSC measurements were performed to obtain a more complete picture of the phase behavior of the different NAC : DPPC molar ratios for the hydrated liposomes. The parameters analyzed in the thermograms obtained were T_m, ΔH_{cal}, $\Delta T_{1/2}$, and ΔS (Table S10, ESI†). The phase-transition temperature, T_m, is the one where the specific heat excess reaches a maximum. For a symmetric curve, T_m represents the temperature at which the transition from the gel to the liquid crystalline state is complete. The area below the DSC thermogram curve is a direct measurement of the calorimetric determination of the phase transition enthalpy, ΔH_{cal}. The cooperative unit (C. U.) is the ratio of the van't Hoff (ΔH_{vH}) and calorimetric enthalpies. The phase transition sharpness is often expressed as the width of the mean height of the main transition, $\Delta T_{1/2}$. The entropic change associated with the phase transition may be calculated with the following formula: $\Delta S = \Delta H_{cal}/T_m$.

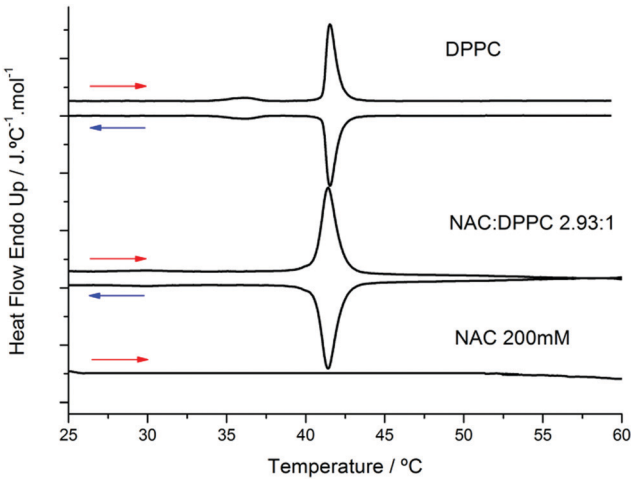

Fig. 8 DSC heating (red arrow) and cooling (blue arrow) scans of DPPC alone; heating and cooling thermograms illustrating the effect of the exposure to high temperature on the thermotropic phase behavior of DPPC multilamellar vesicles at a NAC : DPPC molar ratio of 2.93 : 1 and heating scans of the 200 mM NAC solution.

The calculation of the van't Hoff enthalpy was described in detail by Wojtowicz *et al.*[40–47]

In Fig. 9, we can see the pure DPPC thermogram and the different mixtures, where it is possible to appreciate how these change when the NAC/DPPC molar ratio increased.

The pure DPPC thermogram (Fig. 9) clearly shows two sharp endothermic peaks of different intensities: a lower one at 36.2 °C (T_p) and a higher one at 41.5 °C (T_m), which correspond to the pretransition ($L_{\beta'}$ to $P_{\beta'}$) and main phase transition ($P_{\beta'}$ to L_α), respectively.[45,46] The first peak presents a low transition enthalpy attributed to phospholipid polar head mobility, whereas the second enthalpy was assigned to hydrocarbon chain movement (Table S9, ESI†).

The NAC:DPPC complex at acid pH did not present changes in the transition temperature (T_m), but at physiological pH, this changed slightly toward higher values with respect to the pure lipid, thus stabilizing the gel phase (Table S10, ESI†). Below the main phase transition, large domains of the gel phase were identified by their characteristic striated appearance and highly ordered structure, and in addition, small regions of the lower order (liquid crystalline) assembly could also be observed.[39–46] One of the more intriguing phases is the ripple phase, which is characterized by corrugations in the lipid bilayer with a well-defined periodicity. The ripple phase exists in a temperature range between the pretransition temperature and the main phase transition temperature and is observed only for certain lipid families. The molecular origin of the ripple-phase formation has traditionally been associated with the lipid headgroup region, and for this reason lipids are normally divided into ripple-forming lipids and non-ripple-forming lipids, based on their head groups. One of the families of ripple-forming lipids is the extensively studied phosphatidylcholines.[47]

In the pure DPPC thermogram (Fig. 9), we can see that the peak corresponding to the pretransition at 35.85 °C (T_p) decreased in intensity gradually and moved toward lower

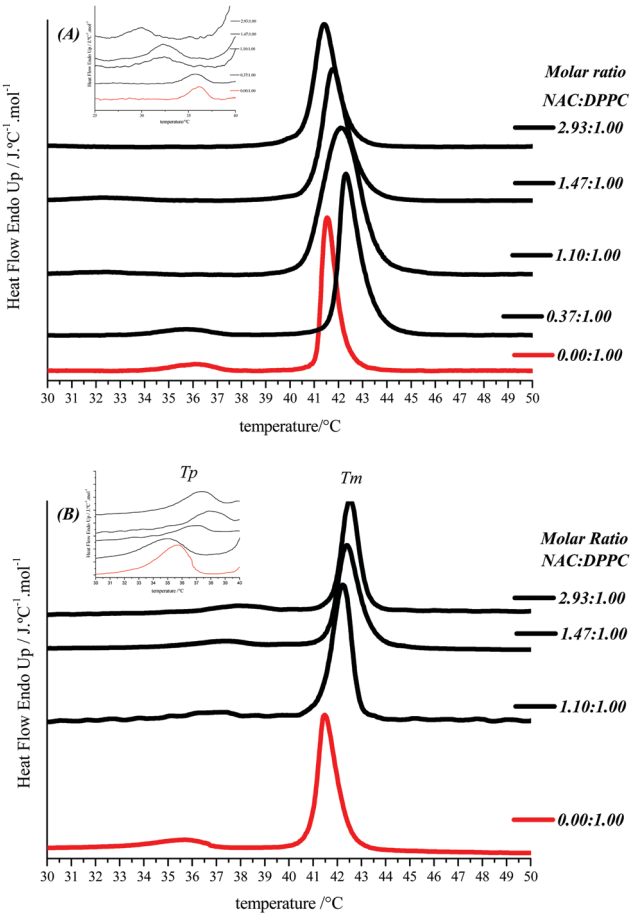

Fig. 9 DSC thermograms of the NAC complex: DPPC at acid (A) and physiological (B) pH, where the main transition temperature (T_m) and the pretransition temperature (T_p) can be observed.

temperatures with the NAC : DPPC molar ratio increasing at pH 2, while at pH 7, T_p increased with respect to the pure lipid, from the molar ratio 1.10 : 1.00 (Table S10, ESI†).

In these systems, both at acidic pH and at physiological pH, the disappearance of T_p was not observed at all molar ratios measured for the NAC : DPPC complex. This behavior is clearly different from that previously reported for the cysteine:DPPC, methyl cysteine:DPPC, and ethyl cysteine:DPPC complexes,[41–43] in which in all of these, T_p disappears when the amino acids interact with the lipid.

Several attempts have been made to explain why ripple phases form. Numerous models share the common idea that ripples result from a periodic local spontaneous curvature in the lipid bilayer. Many different reasons for the origin of this local spontaneous curvature have been suggested, including electrostatic coupling between water molecules and the polar lipid headgroups.[45–47]

In this case we propose that the ripple phases form, not disappear, because there is an electrostatic coupling between NAC molecules and the polar lipid headgroups. This interaction is more significant at physiological pH than at acidic pH, where a lower entropy is observed in the NAC:DPPC complex. Therefore, a more favorable interaction is assumed at physiological pH than at acidic pH.

Experimental studies have indicated the coexistence of gel-state and fluid-state lipids in the ripple phase.[45–47]

The values of the T_p for the different molar ratios of the complex at the two pH studied were coincident between the measurements of FTIR and DSC.[48–50] These results reaffirm the importance of the PO_2^- group as a sensor not only of the state of hydration but also of the formation of new intermolecular bonds, which would lead to the formation of different domains. Therefore, at acidic pH, where T_p decreases, we think that there would be an increase in domains in the gel state, while at physiological pH, a greater amount of domains in the crystalline liquid state should be observed (Tables S9 and S10, ESI†).

We observed an increase in the value of $\Delta T_{1/2}$ as the molar ratio NAC : DPPC increased, which would indicate a loss of the cooperativity of the lipid hydrocarbon chains.[43–46] For this loss of cooperativity, the system NAC:DPPC needs more energy (ΔH_{cal}) to step from the gel state to the liquid crystalline state at acid pH. On the other hand, the value of $\Delta T_{1/2}$ decreases from the molar ratio NAC : DPPC 1.10 : 1.00 with respect to the pure lipid, making cooperativity easier at physiological pH with respect to the behavior at acid pH.

4. Conclusions

The spectroscopic and calorimetric methods employed in this work coincide in the interaction of NAC with the hydrocarbon chains at acid and physiological pH values. These results indicate that NAC did not penetrate this region of the lipid membrane but it produced a slight perturbation at the hydrocarbon region. These results show clearly that the NAC molecules were located in the hydrophilic part of the multilamellar vesicles of DPPC.

At physiological pH, we reported an increase in T_m. This behavior could be an indirect effect of the strong interaction of the amino acid with specific groups of the polar head of the lipid, where the structured water of the interphase (C=O region) would be replaced for NAC molecules with the formation of new hydrogen bonds. The amino acid also produced, in addition to dehydration, the stabilization of the gel state by a new "disordered" arrangement of the hydrocarbon chains. This behavior was not observed at acidic pH, where there were no changes in T_m observed.

It can be inferred that at physiological pH, NAC molecules alter the hydration bilayer in the polar head of the lipid membrane as well as causing changes in the dynamics of the membrane, which may play an important role in the regulation of its properties. This behavior would explain its effect as a strong mucolytic agent. This consideration disputes the idea that lipids act merely as a "solvent" of membrane proteins or as simple supports to compartmentalize biological environments. The vibrational behavior of the groups of the polar head of the lipid reveal the role of the lipid as an oxidant on the thiol site of the NAC.

The results of these studies provide information on membrane integrity and on the physicochemical properties of the lipid bilayer. They also allow us to know the specific interactions with NAC, which is essential for the rational design of lipid drug delivery systems.

Conflicts of interest

There are no conflicts to declare.

Acknowledgements

We thank PIUNT (D0639/1/3), CONICET (PIP 002) of R. Argentina for the research grants. A. Ben Altabef is member of the Research Career of CONICET (R. Argentina). J. M. Arias is fellow of CONICET (R. Argentina).

References

1 J. M. Arias, M. E. Tuttolomondo, S. B. Díaz and A. Ben Altabef, Reorganization of Hydration Water of DPPC Multilamellar Vesicles Induced by L-Cysteine Interaction, *J. Phys. Chem. B*, 2018, **122**, 5193–5204.

2 J. M. Arias, S. B. Díaz, A. Ben Altabef and F. G. Dupuy, Interaction of cysteine and its derivatives with monolayers of Dipalmitoyl phosphatidylcholine, *Colloids Surf., B*, 2019, **184**, 1105482.

3 L. Bonanomi and A. Gazzaniga, Toxicological, pharmacokinetic and metabolic studies on acetylcysteine, *Eur. J. Respir. Dis. Suppl.*, 1980, **111**, 45–51.

4 M. Jones, A. Lawrence, P. Wardman and M. J. Burkitt, Kinetics of superoxide scavenging by glutathione: an evaluation of its role in the removal of mitochondrial superoxide, *Biochem. Soc. Trans.*, 2003, **31**(6), 1337–1339.

5 W. Droge, H. P. Eck and S. Mihm, HIV-induced cysteine deficiency and T-cell dysfunction – a rationale for treatment with N-acetyl cysteine, *Immunol. Today*, 1992, **13**, 211–214.

6 L. A. Herzenberg, S. C. De Rosa, J. G. Dubs, M. Roederer, M. T. Anderson, S. W. Ela and S. C. Deresinski, Glutathione deficiency is associated with impaired survival in HIV disease, *Proc. Natl. Acad. Sci. U. S. A.*, 1997, **94**, 1967–1972.

7 K. R. Atkuri, J. J. Mantovani, L. A. Herzenberg and L. A. Herzenberg, N-acetylcysteine – a safe antidote for cysteine/glutathione deficiency, *Curr. Opin. Pharmacol.*, 2007, **7**(4), 355–359.

8 B. Halliwell, Antioxidants in human health and disease, *Annu. Rev. Nutr.*, 1996, **16**, 33–50.

9 L. Prescott, Oral or Intravenous N-Acetylcysteine for Acetaminophen Poisoning?, *Ann Emerg. Med.*, 2005, **45**, 409–413.

10 R. Tirouvanziam, C. K. Conrad, T. Bottiglieri, L. A. Herzenberg, R. B. Moss and L. A. Herzenberg, High-dose oral N-acetylcysteine, a glutathione prodrug modulates inflammation in cystic fibrosis, *Proc. Natl. Acad. Sci. U. S. A.*, 2006, **103**, 4628–4633.

11 R. A. Cobos Picot, M. Puiatti, A. Ben Altabef, R. Rubira, S. Sánchez-Cortes, S. B. Díaz and M. E. Tuttolomondo, Raman, SERS and UV – Circular Dichroism Spectroscopic study of N-Acetyl-L-Cysteine in Aqueous Solutions, *New J. Chem.*, 2019, **43**, 15201–15212.

12 L. A. Bagatolli, J. H. Ipsen, A. C. Simonsen and O. G. Mouritsen, An outlook on organization of lipids in membranes: searching for a realistic connection with the organization of biological membranes, *Prog. Lipid Res.*, 2010, **49**, 378–389.

13 L. A. Bagatolli and O. G. Mouritsen, *Life-As a Matter of fast Berlin*, Springer-Verlag, Heidelberg, New York, 2015, pp. 1–5.

14 G. A. Senisterra, E. A. Disalvo and J. J. Gagliardino, Osmotic dependence of the lysophosphatidylcholine lytic action on liposomes in the gel state, *Biochim. Biophys. Acta*, 1988, **941**, 264–270.

15 A. D. Bangham, M. W. Hill and N. G. A. Miller, *Methods in Membrane Biology*, Plenum Press, New York, 1974.

16 T. Heimburg, *Thermal Biophysics of Membranes*, Wiley VCH, Berlin, Germany, 2007.

17 A. V. Popova and D. K. Hincha, Thermotropic phase behavior and headgroup interactions of the nonbilayer lipids phosphatidylethanolamine and monogalactosyldiacylglycerol in the dry state, *BMC Biophys.*, 2011, **4**, 1–11.

18 H. H. Mantsch and R. N. McElhaney, Phospholipid phase transitions in model and biological membranes as studied by infrared spectroscopy, *Chem. Phys. Lipids*, 1991, **57**, 213–226.

19 H. L. Casal and H. H. Mantsch, Polymorphic phase behaviour of phospholipid membranes studied by infrared spectroscopy, *Biochim. Biophys. Acta*, 1984, **779**, 381–401.

20 D. G. Cameron, H. L. Casal and H. H. Mantsch, The application of Fourier transforms infrared transmission spectroscopy to the study of model and natural membranes, *J. Biochem. Biophys. Methods*, 1979, **1**, 21–36.

21 D. Bilge, N. Kazanci and F. Severcan, Acyl chain length and charge effect on Tamoxifen-lipid model membrane interactions, *J. Mol. Struct.*, 2013, **1040**, 75–82.

22 C. J. Orendorff, M. W. Ducey and J. E. Pemberton, Quantitative correlation of Raman spectral indicators in determining conformational order in alkyl chains, *J. Phys. Chem.*, 2002, **106**, 6991–6998.

23 B. P. Gaber and W. L. Peticolas, On the quantitative interpretation of biomembrane structure by Raman Spectroscopy, *Biochim. Biophys. Acta*, 1977, **465**, 260–274.

24 C. B. Fox and J. M. Harris, Confocal Raman microscopy for simultaneous monitoring of partitioning and disordering of tricyclic antidepressants in phospholipid vesicle membranes, *J. Raman Spectrosc.*, 2010, **41**, 498–507.

25 C. B. Fox, R. H. Uibel and J. M. Harris, Detecting phase transitions in phosphatidylcholine vesicles by Raman microscopy and self-modeling curve resolution, *J. Phys. Chem. B*, 2007, **111**, 11428–11436.

26 V. Miguel, M. E. Defonsi Lestard, M. E. Tuttolomondo, S. B. Díaz, A. Ben Altabef, M. Puiatti and A. B. Pierini, Molecular view of the interaction of S-methyl methanethiosulfonate with DPPC bilayer, *Biochim. Biophys. Acta, Biomembr.*, 2016, **1858**(1), 38–46.

27 W. Hübner and A. Blume, Interactions at the lipid-water interface, *Chem. Phys. Lipids*, 1998, **96**, 99–123.
28 W. Pohle, C. Selle, H. Fritzsche and H. Binder, Fourier transform infrared spectroscopy as a probe for the study of the hydration of lipid self-assemblies. Methodology and general phenomena, *Biospectroscopy*, 1998, **4**, 267–280.
29 W. Pohle and C. Selle, Fourier-transform infrared spectroscopic evidence for a novel lyotropic phase transition occurring in dioleoylphosphatidylethanolamine, *Chem. Phys. Lipids*, 1996, **82**, 191–198.
30 A. Blume, R. W. Hübne and G. Messner, Fourier transform infrared spectroscopy of $^{13}C{=}O$-labeled phospholipids hydrogen bonding to carbonyl groups, *Biochemistry*, 1988, **27**, 8239–8249.
31 S. B. Díaz, Lysoderivatives Action on Lipidic Membranes in Presence of Sugars Adsorbed at the Interface, PhD dissertation, Universidad Nacional de Tucumán, Tucumán, R. Argentina, 2001.
32 A. H. Lewis and R. N. McElhaney, The structure and organization of phospholipid bilayers as revealed by infrared spectroscopy, *Chem. Phys. Lipids*, 1998, **96**, 9–21.
33 J. L. R. Arrondo, F. M. Goñi and J. M. Macarulla, Infrared spectroscopy of phosphatidylcholines in aqueous suspension a study of the phosphate group vibrations, *Biochim. Biophys. Acta*, 1984, **794**, 165–168.
34 G. L. Jendrasiak and R. L. Smith, The effect of the choline head group on phospholipid hydration, *Chem. Phys. Lipids*, 2001, **113**, 55–66.
35 M. A. Frías, A. Nicastro, N. M. C. Casado, A. M. Gennaro, S. B. Díaz and E. A. Disalvo, Arbutin blocks defects in the ripple phase of DMPC bilayers by changing carbonyl organization, *Chem. Phys. Lipids*, 2007, **14**, 722–729.
36 J. M. Arias, M. E. Tuttolomondo, S. B. Díaz and A. B. Altabef, FTIR and Raman analysis of L-cysteine ethyl ester HCl interaction with dipalmitoylphosphatidylcholine in anhydrous and hydrated states, *J. Raman Spectrosc.*, 2015, **46**, 369–376.
37 J. M. Arias, M. E. Tuttolomondo, S. B. Díaz and A. B. Altabef, Molecular view of the structural reorganization of water in DPPC multilamellar membranes induced by L-cysteine methyl ester, *J. Mol. Struct.*, 2018, **1156**, 360–368.
38 R. N. McElhaney, The use of differential scanning calorimetry and differential thermal analysis in studies of model and biological membranes, *Chem. Phys. Lipids*, 1982, **30**, 229–259.
39 R. Pignatell, *Drug-Biomembrane Interaction Studies: The Application of Calorimetric Techniques*, Woodhead Publishing, 1st edn, 2013, print.
40 K. Wojtowicz, W. I. Gruszecki, W. I. Walicka and M. Barwicz., Efect of amphotericin B on dipalmitoylphosphatidylcholine membranes: calorimetry, ultrasound absorption and monolayer technique studies, *Biochim. Biophys. Acta, Biomembr.*, 1998, **1373**, 220–226.
41 S. M. Ohline, M. L. Campbell, M. T. Turnbull and S. J. Kohler, Differential Scanning Calorimetric Study of Bilayer Membrane Phase Transitions. A Biophysical Chemistry Experiment, *J. Chem. Educ.*, 2011, **78**(9), 251–256.
42 G. Kostantinos, S. Hatziantoniou, V. Kyriakos and D. Costas, Effect of a bioactive curcumin derivative on DPPC membrane: A DSC and Raman spectroscopy study, *Thermochim. Acta*, 2006, **447**, 1–4.
43 R. N. A. H. Lewis, N. Mak and R. N. McElhaney, A differential scanning calorimetric study of the thermotropic phase behavior of model membranes composed of phosphatidylcholines containing linear saturated fatty acyl chains, *Biochemistry*, 1987, **26**, 6118–6126.
44 S. Doniach, A thermodynamic model for the monoclinic (ripple) phase of hydrated phospholipid bilayers, *J. Chem. Phys.*, 1979, **70**, 4587–4596.
45 T. Kaasgaard, C. Leidy, J. H. Crowe, O. G. Mouritsen and K. Jørgensen, Temperature-Controlled Structure and Kinetics of Ripple Phases in One- and Two-Component Supported Lipid Bilayers, *Biophys. J.*, 2003, **85**, 350–360.
46 W. J. Sun, S. Tristram-Nagle, R. M. Suter and J. F. Nagle, Structure of the ripple phase in lecithin bilayers, *Proc. Natl. Acad. Sci. U. S. A.*, 1996, **93**, 7008–7012.
47 M. Rappolt, G. Pabst, G. Rapp, M. Kriechbaum, H. Amenitsch, C. Krenn, S. Bernstorff and P. Laggner, New evidence for gel-liquid crystalline phase coexistence in the ripple phase of phosphatidylcholines, *Eur. Biophys. J.*, 2000, **29**, 125–133.
48 F.-G. Wu, N.-N. Wang, L.-F. Tao and Z.-W. Yu, Acetonitrile Induces Nonsynchronous Interdigitation and Dehydration of Dipalmitoylphosphatidylcholine Bilayers, *J. Phys. Chem. B*, 2010, **114**, 12685–12691.
49 F.-G. Wu, Q. Jia, R.-G. Wu and Z.-W. Yu, Regional Cooperativity in the Phase Transitions of Dipalmitoylphosphatidylcholine Bilayers: The Lipid Tail Triggers the Isothermal Crystallization Process, *J. Phys. Chem. B*, 2011, **115**, 8559–8568.
50 F.-G. Wu, R.-G. Wu, H.-Y. Sun, Y.-Z. Zheng and Z.-W. Yu, Demixing and crystallization of DODAB in DPPC–DODAB binary mixtures, *Phys. Chem. Chem. Phys.*, 2014, **16**, 15307–15318.

